

Ultra-long organic RTP host-guest doped systems based on pure 4-(1H-imidazole-1-yl)methyl benzoate as versatile hosts

Xiaoxiao Jiao,^{#a} Wenlei Zhang,^{#a} Jieru Zhi,^a Yingxin Wang,^a Mengyao Wang,^a Zhongyi Liu^{*a} and Jinpeng Li^{*a}

^aCollege of Chemistry and Green Catalysis Center, Zhengzhou University, Zhengzhou, Henan 450001, P. R. China.

[#]Xiaoxiao Jiao and Wenlei Zhang contributed equally to this work.

General Information and Materials. All the materials and reagents were obtained from commercial channels and were analytically pure. The host 4-(1H-imidazole-1-yl)methyl benzoate (**MIBA**) was purchased from two companies, namely Jilin Chinese Academy of Sciences - Yanshen Company and Zhengzhou Anmusi Company. The guest imidazole-4,5-dicarboxylic acid (**IDBA**), 1,2,3-triazole-4,5-dicarboxylic acid (**TDCA**) and 1,3-benzenedicarboxylic acid (**IPA**) were purchased from Zhengzhou Anmusi Company, 3-(1H-imidazol-1-yl)benzoic acid (**m-HIBA**), 3-(4H-1,2,4-triazole-4-yl)benzoic acid (**HTBA**) and 5-(1H-imidazol-1-yl)isophthalic acid (**H₂IMIP**) were purchased from Jinan Henghua technology company. The Bruker Tensor 27 infrared spectrometer was used to measure the infrared spectrum (IR) of the sample using potassium bromide pressed in the wavelength range of 400-4000 cm⁻¹. Purity was detected by Waters E2695 high performance liquid chromatography (HPLC) (mobile phase at 70/30 methanol-water ratio (v/v), flow rate 1.0 mL/min, column temperature 35°C, detection wavelength 260 nm). Elemental analysis was performed on the elemental analyzer FLASH EA 1112. X-ray Powder Diffraction (PXRD) is tested on Panalytical X'pert PRO (Cu-Kα rays)(λ = 1.5418 Å). The fluorescence and phosphorescence spectra of the samples were measured by HITACHI F-4600 fluorescence spectrometer. The Edinburgh FLS980 steady-state transient fluorescence spectrometer was used to measure the phosphorescence/fluorescence lifetime and quantum yield at room temperature. ¹H NMR spectra were obtained on Bruker DRX (400 MHz). The photoluminescent images were taken by an iPhone under a handheld

light. The UV-Vis absorption spectrum was measured by TU-1901 double beam UV-Vis spectrophotometer.

How to make the logo icon. First, we use the toner printer (Printer model: HP LaserJet Professional M1136 MFP) to print the logo on a smooth piece of paper, utilize the tape to stick the logo down, then sprinkle the powder on the tape, finally, we get the logo “crab”.

Crystal Data Collection and Refinement. Crystal data for **MIBA** and **HIBA** were collected at $298\pm 1\text{K}$ using a Bruker APEX-II CCD diffractometer (molybdenum-potassium alpha ray, $\lambda = 0.71073 \text{ \AA}$). The structures of the two crystals were solved using the SHELXS-97 crystallography software package and optimized using the full matrix least squares method by the SHELXL-2014 program.^{1,2}

Synthesis of (MIBA)_n (named MIBA). Pure or crude **Y-MIBA** (60 mg, 0.3 mmol) was added into a 50 mL flask with 20 mL methanol, then stirred until dissolved. After heated in 60°C for 24h, the insoluble material was filtered out, at the same time, the solution was sealed into different cilin bottles for three days, a large number of colorless transparent needle crystals were obtained. The crystals of **MIBA** were filtered and dried in the air at room temperature (yield: 92%, based on **MIBA**). Elemental Anal. Calcd for $\text{C}_{2.75}\text{H}_{2.5}\text{N}_{0.5}\text{O}_{0.5}$: C, 65.34; H, 4.95; N, 13.86%. Found: C, 66.52; H, 4.57; N, 13.80%. IR (KBr pellet, cm^{-1}): 3397s, 3142m, 3110s, 2954m, 2842s, 1924s, 1715s, 1609s, 1526s, 1483s, 1434s, 1311s, 1267m, 1062s, 961s, 769m, 650s, 507m.

Synthesis of (HIBA)_n (named HIBA). **HIBA** (30 mg, 0.159 mmol) was added into a 25 mL flask with 7.5 mL water and 7.5 mL methanol, heated in 75°C for 40 min with stirring, then cooled to room temperature, a large number of colorless transparent needle crystals were precipitated. The crystals were filtered and dried in the air at ambient temperature (yield: 55%, based on **HIBA**).³ Element Anal. Calcd for $\text{C}_{10}\text{H}_8\text{N}_2\text{O}_2$: C, 63.83; H, 4.29; N, 14.89%. Found: C, 63.76; H, 4.25; N, 14.87%. IR (KBr pellet, cm^{-1}): 3437s, 3159m, 3117m, 2409s, 1930s, 1697s, 1606s, 1527s, 1304m, 1056s, 959s, 835s.

Structural description of $(\text{MIBA})_n(\text{MIBA})$.

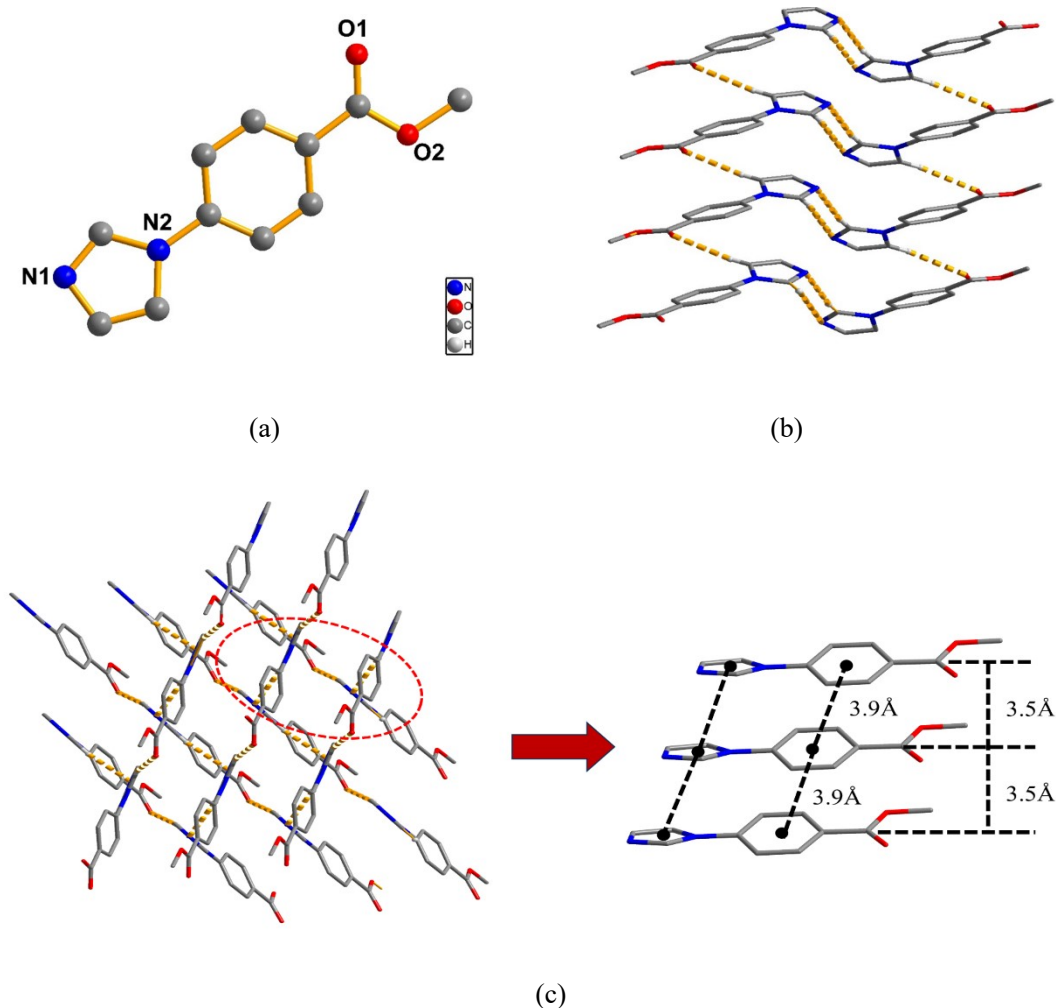


Figure S1. (a) The asymmetric unit of $(\text{MIBA})_n(\text{MIBA})$ crystal; (b) The 1D planar structure; (c) 2D structure constructed *via* 1D $\pi \cdots \pi$ stacking.

The structure of pure and crude $(\text{MIBA})_n$ crystals remains identical. The single crystal X-ray shows that $(\text{MIBA})_n$ is monoclinic and the space group belongs to $P1(2)1(1)$. As shown in Figure S1a, there is the asymmetric unit of the $(\text{MIBA})_n$, which contains a carboxylic group. As shown in Figure S1b, on the ac plane, the ligand molecules $(\text{MIBA})_n$ are mainly connected by intermolecular hydrogen bonds between $\text{C3-H3} \cdots \text{O1}$ [$\text{H3} \cdots \text{O1} = 2.63(2) \text{ \AA}$, $\angle \text{C3-H3} \cdots \text{O1} = 170.8(8)^\circ$] and $\text{C1-H1} \cdots \text{N1}$ [$\text{H1} \cdots \text{N1} = 2.54(2) \text{ \AA}$, $\angle \text{C1-H1} \cdots \text{N1} = 170.9(8)^\circ$] to form a 1D layered structure, and the layers are stacked infinitely by $\pi \cdots \pi$ stacking between the benzene rings and imidazole rings (Figure S1c, the distance between two parallel $(\text{MIBA})_n$ molecules'

benzene/imidazole cores is 3.9 Å, the perpendicular distance is 3.5 Å, and the angle is 68°).

Structural description of $(\text{HIBA})_n$ (HIBA).

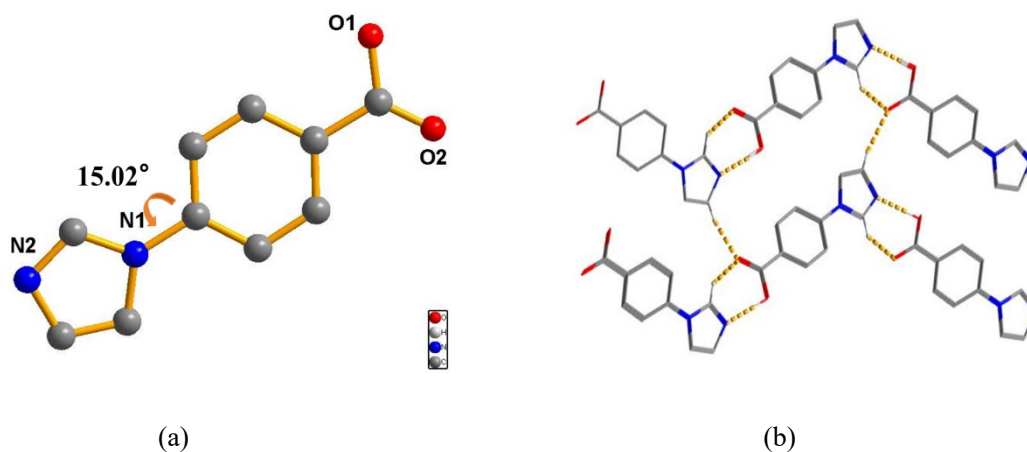


Figure S2. (a) The asymmetric unit of HIBA crystal; (b) The 2D planar structure.

The single crystal X-ray shows that $(\text{HIBA})_n$ is monoclinic and the space group belongs to $Pn(7)$.³ As shown in Figure S2a, there is a torsion Angle of 15.02° between imidazole ring and benzene ring in $(\text{HIBA})_n$. On the bc surface, it is mainly composed of intermolecular hydrogen bonds $\text{C3-H3}\cdots\text{O1}$ [$\text{H3}\cdots\text{O1} = 2.54(9) \text{ \AA}$, $\angle\text{C3-H3}\cdots\text{O1} = 117.5(5)^\circ$], $\text{O2-H2}\cdots\text{N1}$ [$\text{H2}\cdots\text{N1} = 1.79(7) \text{ \AA}$, $\angle\text{O2-H2}\cdots\text{N1} = 177.8(5)^\circ$] and $\text{C2-H2A}\cdots\text{O1}$ [$\text{H2A}\cdots\text{O1} = 2.38(7) \text{ \AA}$, $\angle\text{C2-H2A}\cdots\text{O1} = 167.3(8)^\circ$](Figure S2b).

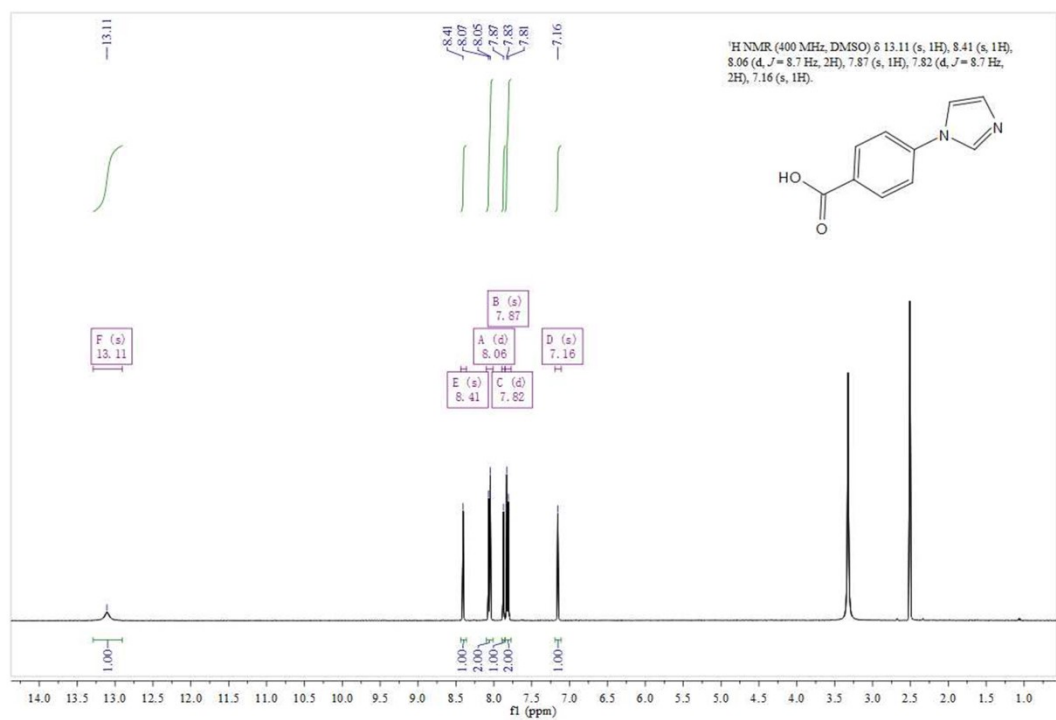


Figure S3. ¹H NMR spectrum impurity **HIBA** [δ_{H} (400 MHz, DMSO-*d*₆) 13.11(OH, 1H, s), 8.41(imz-H, 1H, s), 8.05 (Ph-H, 2H, d, J 8.7), 7.83 (imz-H, 1H, s), 7.81 (Ph-H, 2H, d, J 8.7), 7.16 (imz-H, 1H, s)].

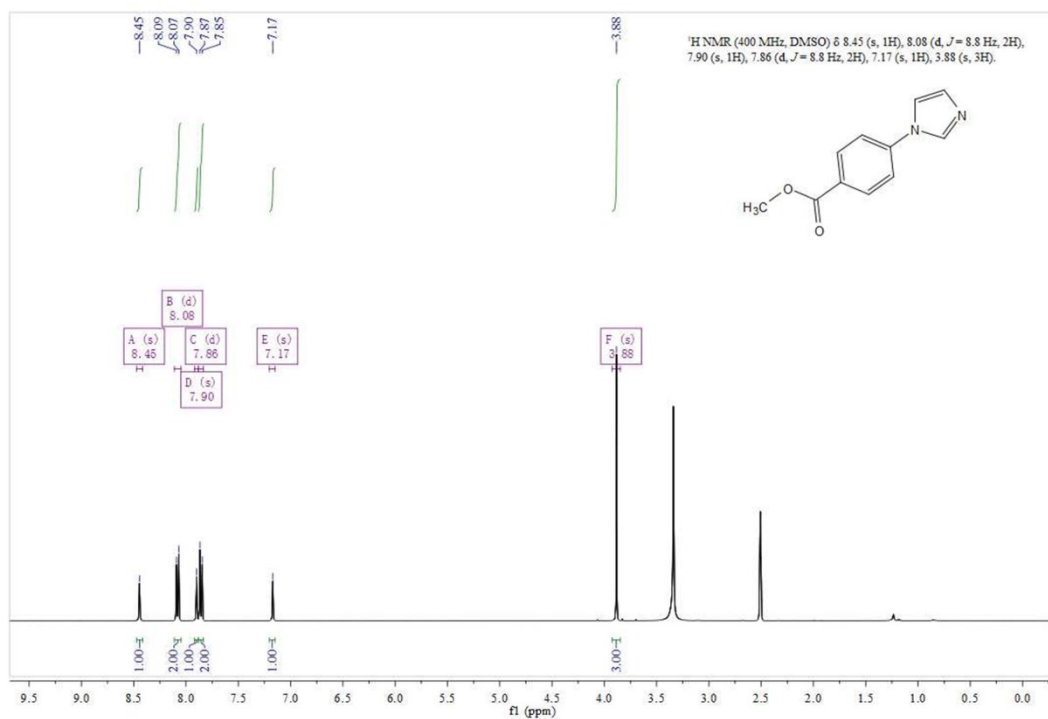


Figure S4. ¹H NMR spectrum of pure MIBA [δ_{H} (400 MHz, DMSO-*d*₆) 8.45 (imz-H, 1H, s), 8.08 (Ph-H, 2H, d, *J* 8.7), 7.90 (imz-H, 1H, s), 7.86 (Ph-H, 2H, d, *J* 8.7), 7.17 (imz-H, 1H, s), 3.88 (CH₃, 3H, s)].

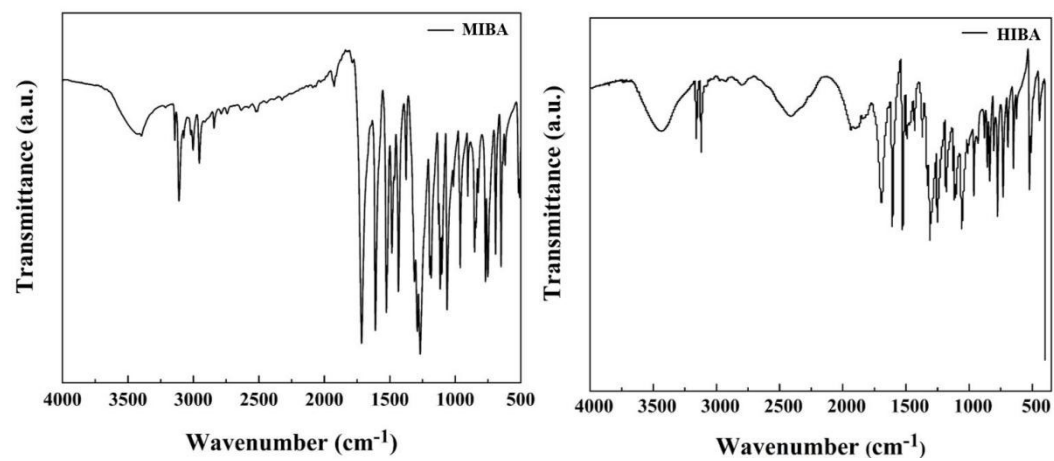


Figure S5. IR spectra of **MIBA** and **HIBA**.

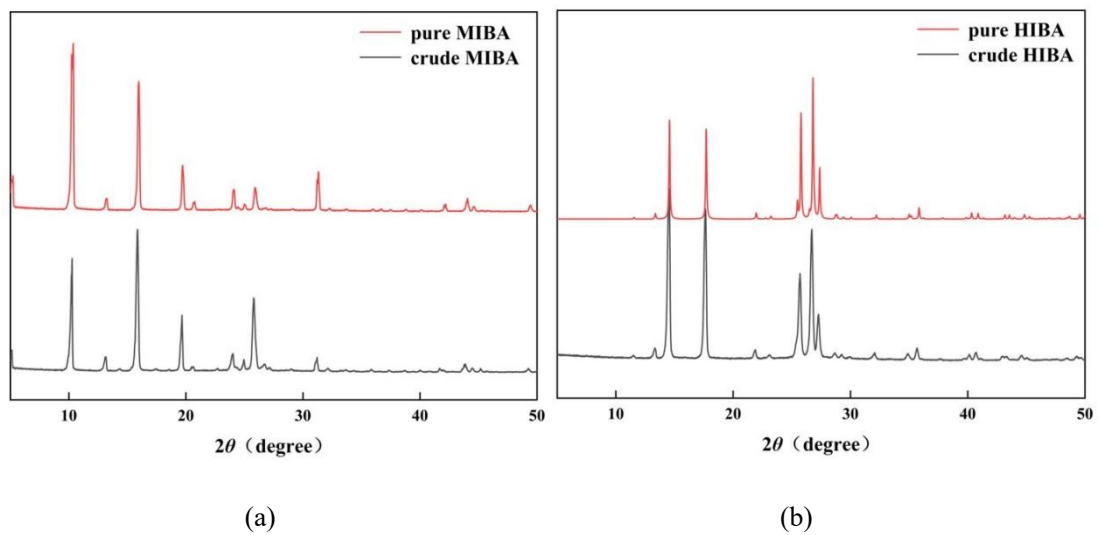


Figure S6. (a) PXRD pattern of curde and pure **MIBA**; (b) PXRD pattern of curde and pure **HIBA**.

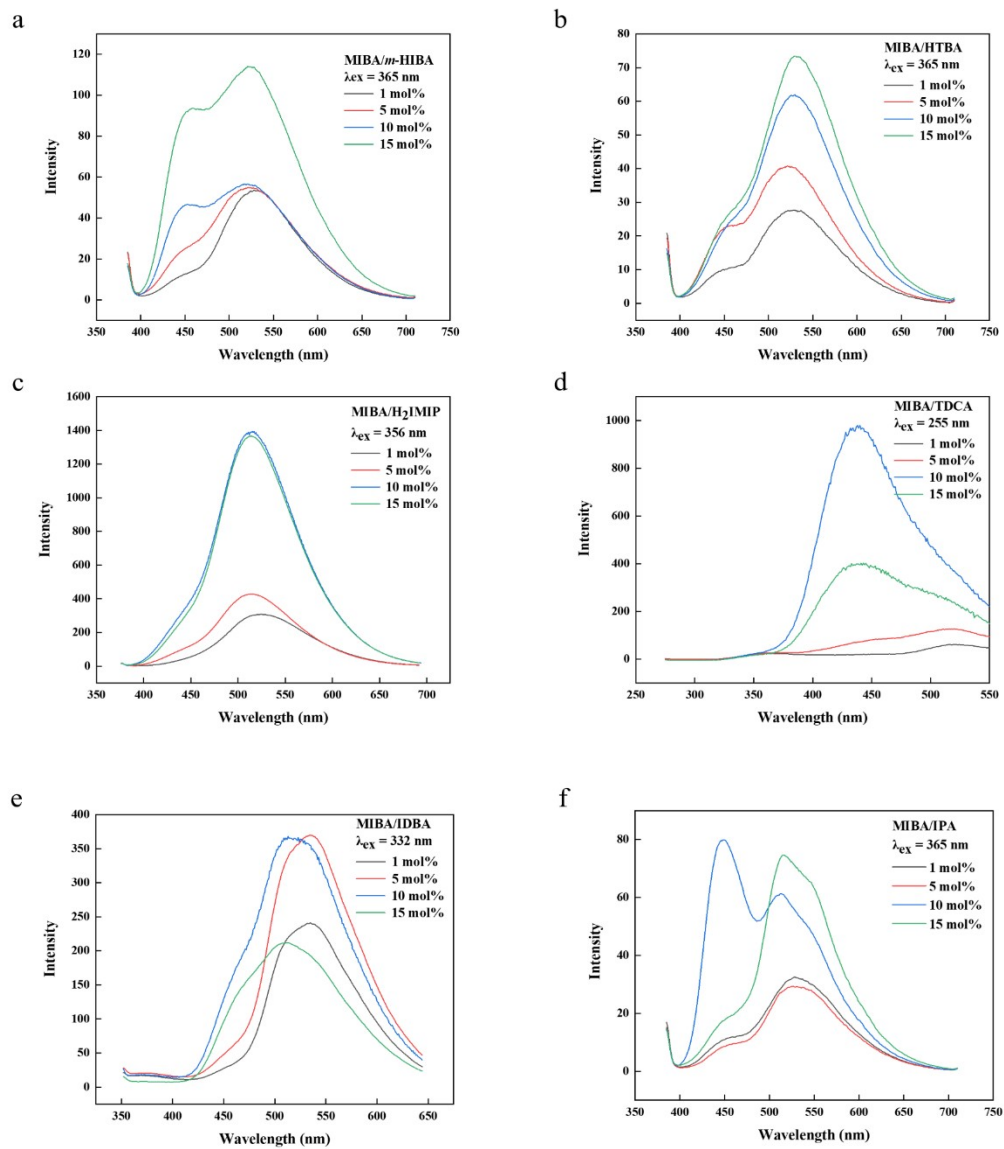


Figure S7. (a)-(f) Phosphorescence emission spectra of **MIBA/*m*-HIBA**, **MIBA/HTBA**, **MIBA/H₂IMIP**, **MIBA/TDCA**, **MIBA/IDBA** and **MIBA/IPA** systems with different doping ratios at room temperature.

Figure S8. (a)-(e) Fluorescence emission spectra of **MIBA/HIBA**, **MIBA/*m*-HIBA**, **MIBA/HTBA**, **MIBA/H₂IMIP**, **MIBA/IDBA**, **MIBA/TDCA** and **MIBA/IPA** at room temperature.

The fluorescence emission spectra of the seven systems were tested at the excitation wavelength of 280 nm. For **MIBA/HIBA** system, when the ratio is 2 mol%, the fluorescence emission intensity reaches the maximum, but when the ratio increases, the fluorescence emission intensity begins to decrease gradually. For **MIBA/m-HIBA** and **MIBA/HTBA** systems, with the increase of doping ratio, the fluorescence intensity decreases gradually, and the emission wavelength also shows different degrees of redshift. For **MIBA/H₂IMIP**, **MIBA/IDBA**, **MIBA/TDCA** and **MIBA/IPA** systems, the fluorescence luminescence intensity also gradually decreases with the increase of doping ratio, and the emission wavelength is basically stable at about 370 nm.

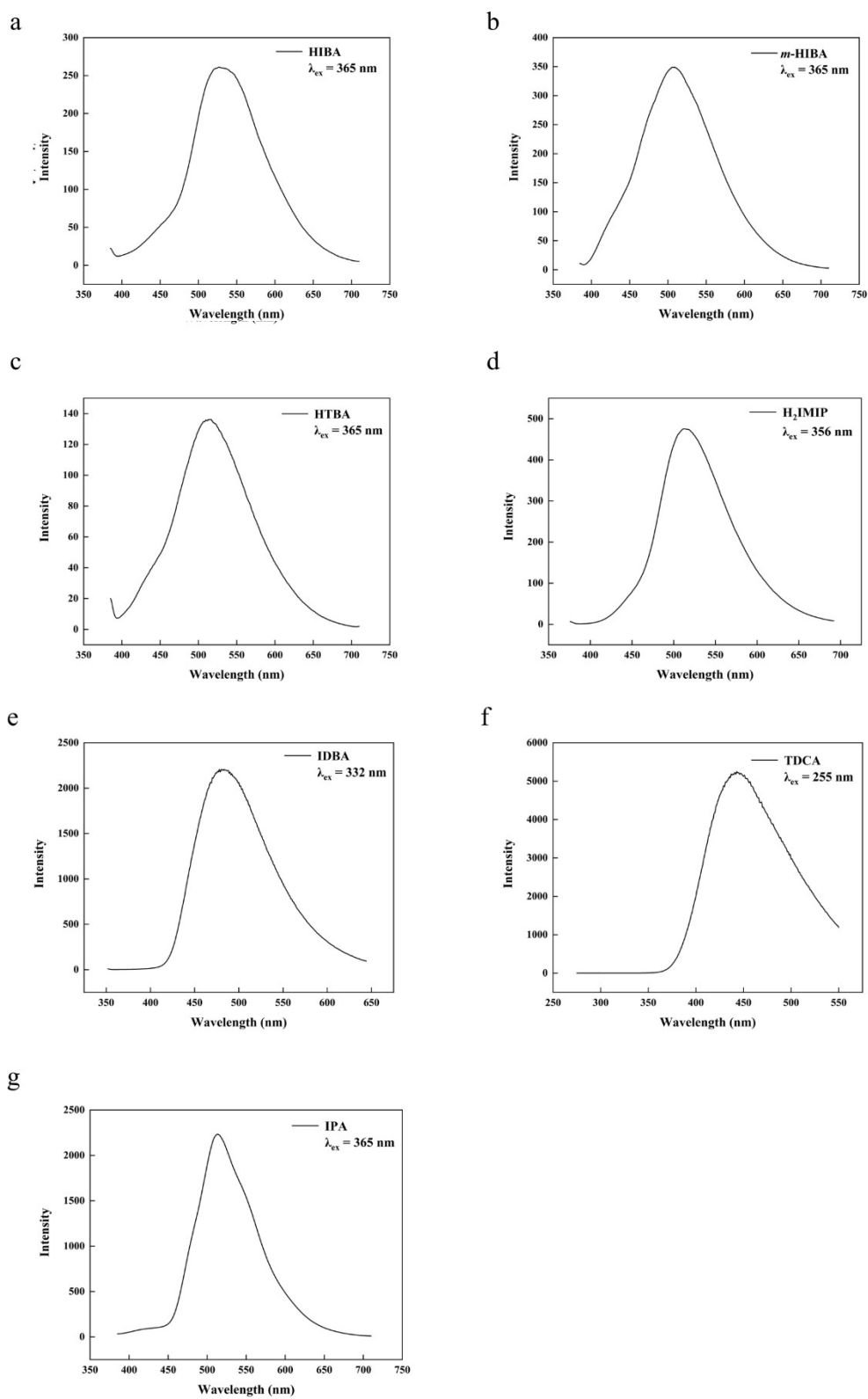
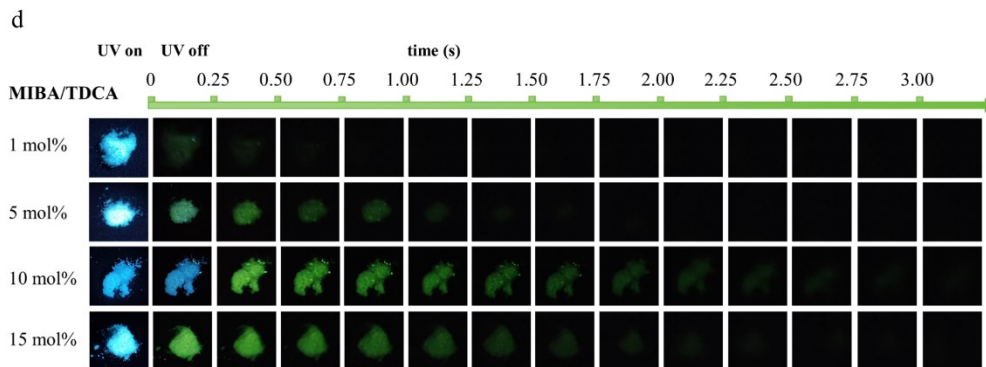
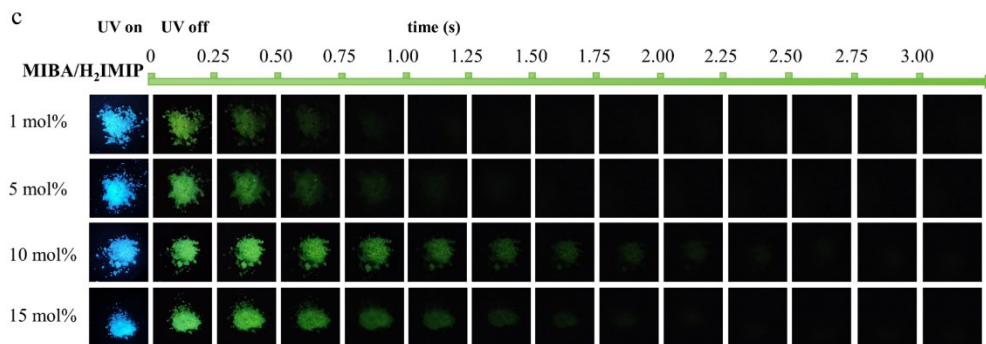
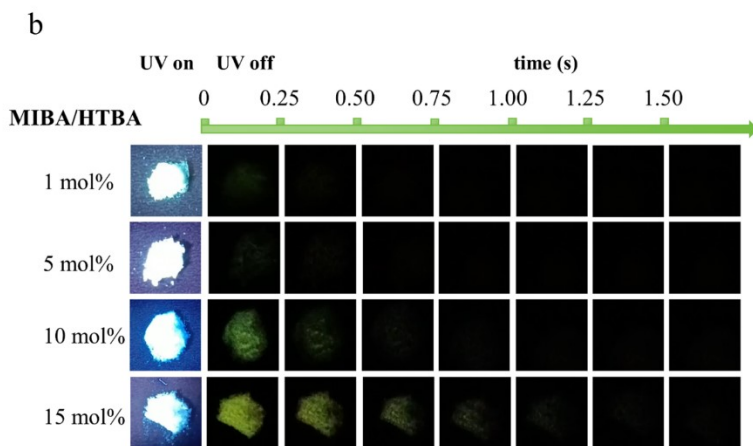
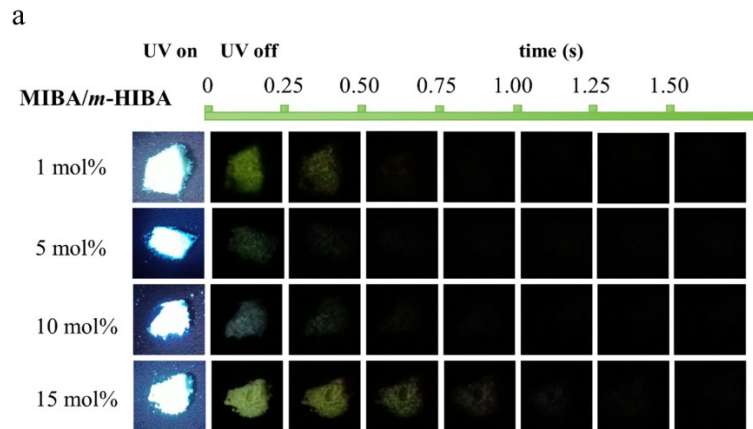


Figure S9. (a)-(g) Phosphorescence emission spectra of **HIBA**, *m*-**HIBA**, **HTBA**, **H₂IMIP**, **IDBA**, **TDCA** and **IPA** monomers at room temperature.



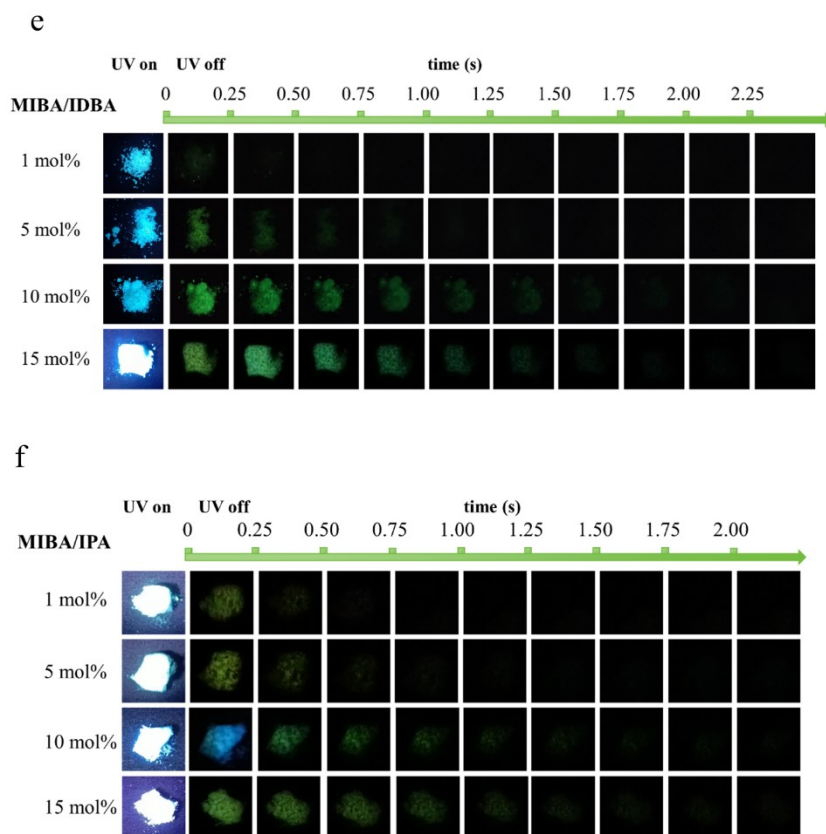


Figure S10. (a)-(f) the afterglow photos of the MIBA/*m*-HIBA, MIBA/HTBA, MIBA/H₂IMIP, MIBA/TDCA, MIBA/IDBA and MIBA/IPA materials with various doping ratios irradiated by a handheld 365 nm UV lamp at room temperature.

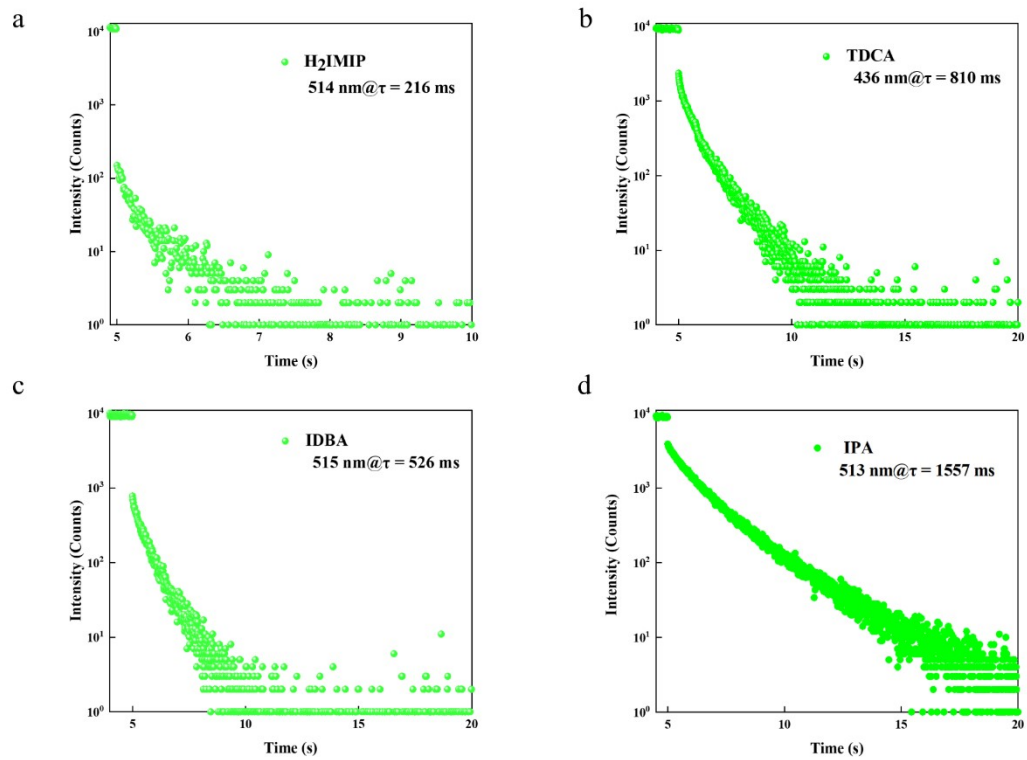


Figure S11. (a)-(d) RTP lifetimes of H_2IMIP , TDCA, IDBA and IPA monomers.

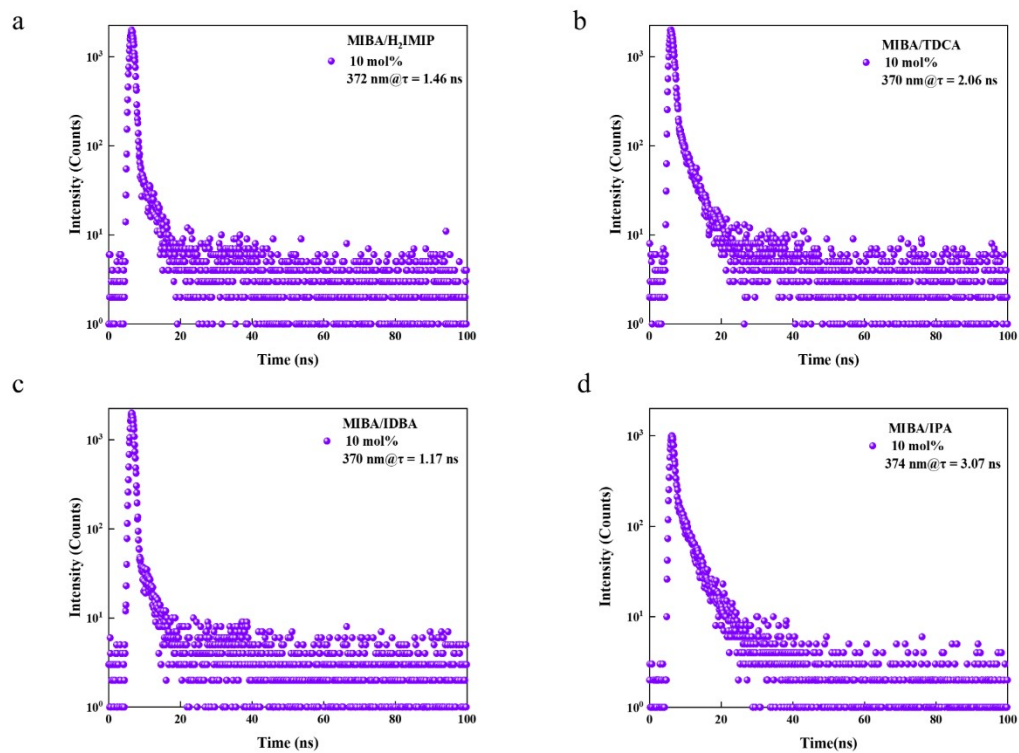


Figure S12. (a)-(d) MIBA/H₂IMIP, MIBA/TDCA, MIBA/IDBA and MIBA/IPA when doping for 10 mol % of fluorescent lifetimes at room temperature ($\lambda_{\text{ex}} = 330$ nm).

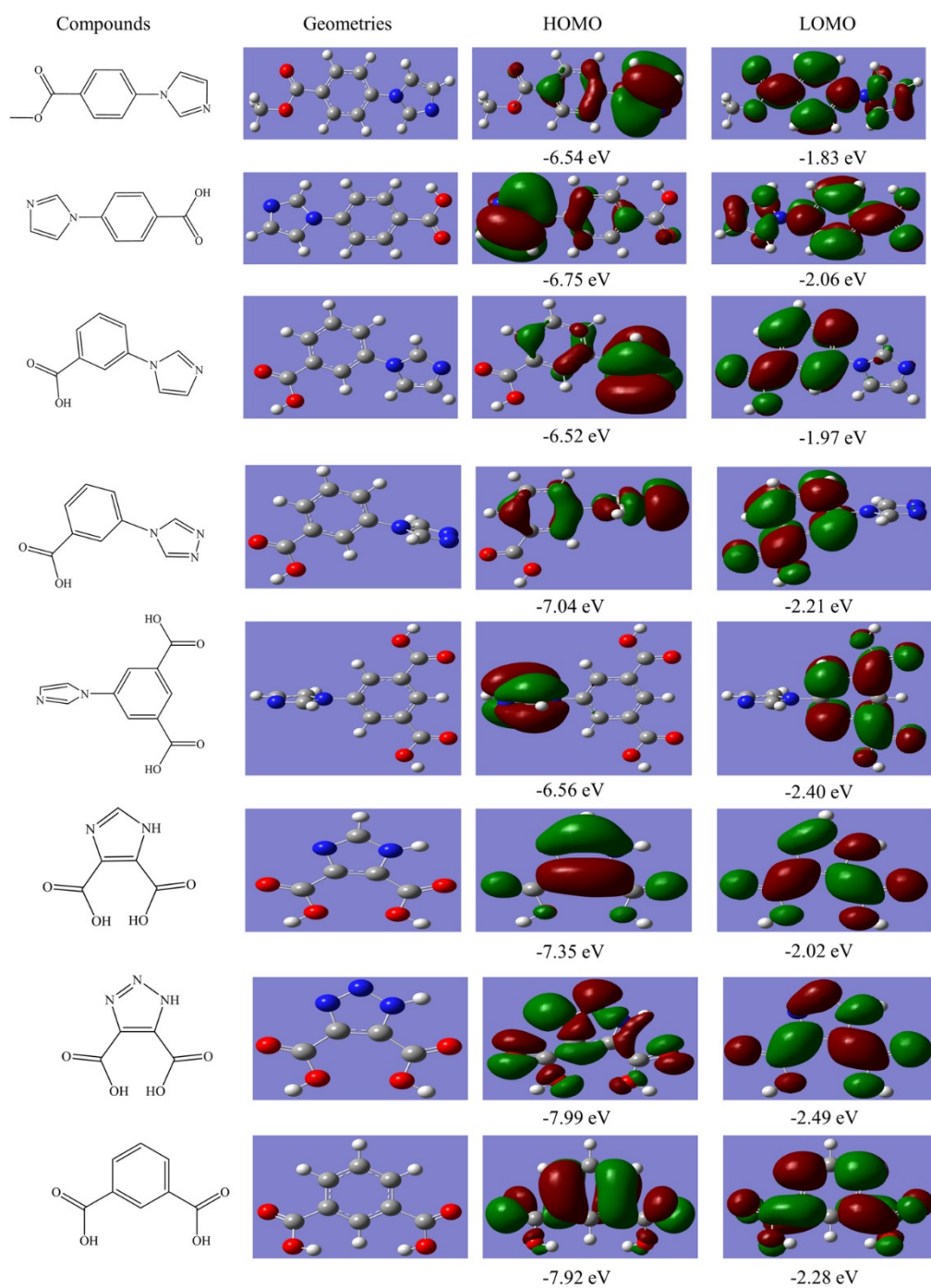


Figure S13. Gaussian16 software package was used to calculate the optimized geometry, HOMO and LOMO at the B3LYP/6-311g(d) theoretical level.⁴⁻⁷

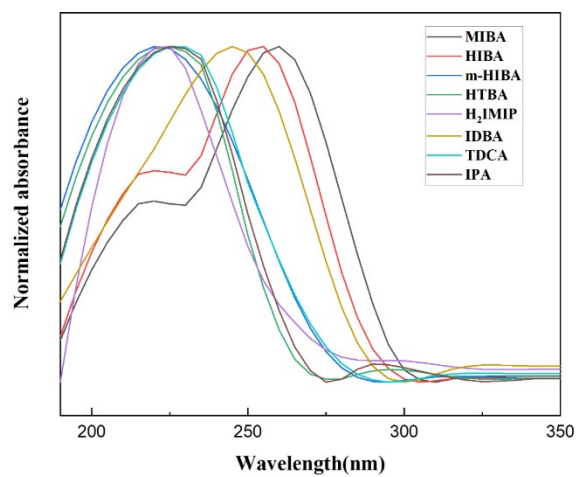


Figure S14. UV absorption spectra of **MIBA**, **HIBA**, **m-HIBA**, **HTBA**, **H₂IMIP**, **IDBA**, **TDCA** and **IPA** in anhydrous methanol.

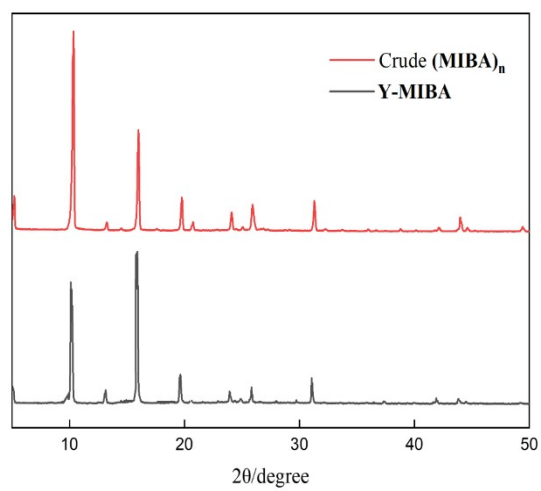


Figure S15. PXRD pattern of crude (MIBA)_n and Y-MIBA.

Table S1. (MIBA)_n and (HIBA)_n crystals parameters

Polymers	(MIBA) _n	(HIBA) _n
Formula	C ₁₁ H ₁₀ N ₂ O ₂	C ₁₀ H ₈ N ₂ O ₂
Fw	202.2	188.1
Temp(K)	293(2)	293(2)
Wavelength(Å)	0.7103	0.7107
Crystal syst	Monoclinic	Monoclinic
Space group	<i>P2₁</i>	<i>Pn</i>
<i>a</i> (Å)	3.9005(4)	4.1240(9)
<i>b</i> (Å)	7.2565(6)	6.6158(14)
<i>c</i> (Å)	17.1927(1)	15.347(3)
<i>α</i> (deg)	90	90
<i>β</i> (deg)	94.660(3)	94.222(7)
<i>γ</i> (deg)	90	90
<i>V</i> (Å ³)	485.0(1)	417.5(8)
<i>Z</i>	8	8
Dc(g·cm ⁻³)	1.385	1.497

F(000)	212	196
θ range for data collection(deg)	3.049~27.442	2.662~27.069
Reflections collected /unique	10045/2168	5298/1619
Data / restraints / params	2168/1/137	1619/2/128
Goodness-of-fit on F ²	1.005	1.120
Final R1 ^a , wR2 ^b	0.0754, 0.0945	0.0795, 0.1655

^a $R_1 = \frac{\sum (|F_o| - |F_c|)}{\sum |F_o|}$. ^b $wR_2 = \frac{[\sum w(|F_o^2| - |F_c^2|)^2]}{[\sum w|F_o^2|]^2}]^{1/2}$.

Table S2. The singlet and triplet excited state transition configurations obtained by TD-DFT calculations [B3LYP/6-311g(d)].

Compounds	States	Energy (eV)	Transition configuration (%)
MIBA	S ₁	4.1601	H→L(97%)
	T ₅	4.4369	H-4→L(53%) H-3→L+1(29%)
	T ₄	4.4238	H-4→L(35%) H-3→L+1(45%) H-1→L(8%)
	T ₃	4.2853	H-3→L(68%) H-2→L(8%) H-1→L+1(12%) H→L+1(9%)
	T ₂	3.6889	H-1→L(36%) H→L(35%) H→L+2(18%)
	T ₁	3.3028	H-3→L+1(9%) H-1→L(37%) H→L(43%)
TDCA	S ₁	4.5291	H-1→L(94%)
	T ₅	4.8506	H-4→L(39%) H-3→L(19%) H-1→L+1(18%)
	T ₄	4.6077	H-3→L(45%) H-1→L+1(38%)
	T ₃	4.2231	H-2→L(47%) H→L(29%) H→L+1(13%)
	T ₂	4.2231	H-1→L(84%)
	T ₁	3.7179	H-2→L(36%) H→L(57%)
H₂IMIP	S ₁	3.6065	H→L(99%)
	T ₅	4.0256	H-3→L(38%) H-1→L+1(47%) H→L+2(5%)
	T ₄	3.8166	H-1→L(63%) H→L(33%)

	T ₃	3.6937	H-3→L(15%) H→L+1(50%) H→L+2(20%) H→L+5(5%)
	T ₂	3.3650	H-1→L(30%) H→L(66%)
	T ₁	3.2882	H-6→L+1(7%) H-3→L(42%) H-1→L+1(26%) H→L+1(19%)
IDBA	S ₁	4.6913	H-2→L(4%) H-1→L(77%) H→L(12%)
	T ₅	5.1122	H-5→L(13%) H-5→L+1(14%) H-4→L(45%) H→L+1(15%)
	T ₄	4.9016	H-6→L(4%) H-3→L(84%)
	T ₃	4.4984	H-4→L(7%) H-2→L(84%)
	T ₂	4.3534	H-1→L(86%) H-1→L+1(6%)
	T ₁	3.4214	H→L(95%)
IPA	S ₁	4.8003	H-1→L+1(30%) H→L(69%)
	T ₅	4.4563	H-3→L(66%) H-2→L+1(26%) H-2→L+2(5%)
	T ₄	4.2777	H-3→L+1(22%) H-3→L+2(5%) H-2→L(70%)
	T ₃	4.2795	H-1→L(33%) H→L+1(54%)
	T ₂	4.0470	H-1→L+1(6%) H→L(92%)
	T ₁	3.4382	H-1→L(66%) H→L+1(31%)

Table S3. Room temperature fluorescence and phosphorescence lifetimes of **MIBA/H₂IMIP**, **MIBA/TDCA**, **MIBA/IDBA** and **MIBA/IPA** at doping of 10 mol% and **H₂IMIP**, **TDCA**, **IDBA** and **IPA**.

Complexes	Fluorescence			Phosphorescence			
	λ_{ex} (nm)	λ_{em} (nm)	τ (ns)	λ_{ex} (nm)	λ_{em} (nm)	τ (ms)	Φ_{Phos} (%)
MIBA/H₂IMIP	330	372	1.46			309	4.03
H₂IMIP	—	—	—	356	514	216	—
MIBA/TDCA	330	370	2.06			1139	0.31
TDCA	—	—	—	255	436	810	—
MIBA/IDBA	330	370	1.17			463	0.11
IDBA	—	—	—	322	515	526	—
MIBA/IPA	330	374	3.07			566	3.50
IPA	—	—	—	365	513	1157	—

Table S4. Photophysical parameters of crude **(MIBA)_n** and **Y-MIBA**.

Sample	$\lambda_{\text{Phos}}(\text{nm})$	$\tau(\text{s})$	$\Phi_{\text{Phos}}(\%)$	$k_{\text{r}}^{\text{Phos}}(\text{s}^{-1})$	$k_{\text{nr}}^{\text{Phos}}(\text{s}^{-1})$
Crude (MIBA)_n	553	0.978	1.28	0.013	1.009
Y-MIBA	531	0.300	0.80	0.026	3.307

$$k_{\text{r}}^{\text{Phos}} = \Phi_{\text{Phos}} / \tau_{\text{Phos}}; k_{\text{nr}}^{\text{Phos}} = (1 - \Phi_{\text{Phos}}) / \tau_{\text{Phos}}.$$

Reference:

- 1 G. M. Sheldrick, A short history of SHELX, *Acta Crystallographica a-Foundation and Advances*, 2008, **64**, 112-122.
- 2 G. M. Sheldrick and T. R. Schneider, in *Methods in Enzymology*, Academic Press, 1997, **277**, 319-343.
- 3 Z. Zheng, W. Q. Geng, Z. C. Wu and H. P. Zhou, 4-(Imidazol-1-yl)benzoic acid, *Acta Crystallographica Section E-Structure Reports Online*, 2011, **67**, O524-U2046.
- 4 P. J. Stephens, F. J. Devlin, C. F. Chabalowski and M. J. Frisch, Ab initio calculation of vibrational absorption and circular dichroism spectra using density functional force fields, *The Journal of Physical Chemistry*, 1994, **98**, 11623-11627.
- 5 W. J. Hehre, R. Ditchfield and J. A. Pople, Self-consistent molecular orbital methods. XII. further extensions of gaussian-type basis sets for use in molecular orbital studies of organic molecules, *The Journal of Chemical Physics*, 1972, **56**, 2257-2261.
- 6 J. D. Dill and J. A. Pople, Self-consistent molecular orbital methods. XV. extended gaussian-type basis sets for lithium, beryllium, and boron, *The Journal of Chemical Physics*, 1975, **62**, 2921-2923.
- 7 B. Ding, L. Ma, Z. Huang, X. Ma and H. Tian, Engendering persistent organic room temperature phosphorescence by trace ingredient incorporation, *Science Advances*, 2021, **7**, eabf9668.